

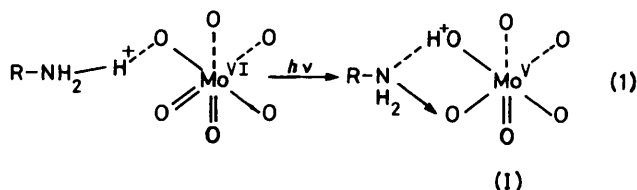
Crystallographic Characterization of the Polyoxotungstate $[\text{Eu}_3(\text{H}_2\text{O})_3(\text{SbW}_9\text{O}_{33})(\text{W}_5\text{O}_{18})_3]^{18-}$ and Energy Transfer in its Crystalline Lattices

Toshihiro Yamase,* Haruo Naruke, and Yoh Sasaki

Research Laboratory of Resources Utilization, Tokyo Institute of Technology, 4259 Nagatsuta, Midori-ku, Yokohama 227, Japan

The potassium salt of the new mixed-polyoxotungstate anion $[\text{Eu}_3(\text{H}_2\text{O})_3(\text{SbW}_9\text{O}_{33})(\text{W}_5\text{O}_{18})_3]^{18-}$ (1) has been prepared from WO_3 , Sb_2O_3 , $\text{Eu}(\text{NO}_3)_3 \cdot 6\text{H}_2\text{O}$, and KOH in water and isolated in crystalline form as $\text{K}_{15}\text{H}_3[\text{Eu}_3(\text{H}_2\text{O})_3(\text{SbW}_9\text{O}_{33})(\text{W}_5\text{O}_{18})_3] \cdot 25.5\text{H}_2\text{O}$. It crystallizes in the monoclinic space group $C2/m$, with $a = 30.250(7)$, $b = 18.568(5)$, $c = 22.101(6)$ Å, $\beta = 109.19(8)^\circ$, and $Z = 4$. A central $\text{Eu}_3(\text{H}_2\text{O})_3$ core is co-ordinated by a B-type α - $\text{SbW}_9\text{O}_{33}$ unit and three W_5O_{18} units with tetrahedral conformation. Each Eu^{3+} in the core exhibits eight-co-ordination by oxygen atoms belonging to H_2O , $\text{SbW}_9\text{O}_{33}$, and W_5O_{18} units. The intramolecular energy transfer from the $\text{O} \rightarrow \text{W}$ charge-transfer levels for the polyoxotungstate crystalline lattices to the emitting $^5\text{D}_0$ level of Eu^{3+} takes place efficiently at least over 6.9 Å which is the largest distance between W and Eu atoms in the anion. A comparison of the lifetime and quantum yield of the emission among (1), $[\text{Eu}(\text{W}_5\text{O}_{18})_2]^{9-}$, and $[\text{Eu}(\text{SiW}_{11}\text{O}_{39})_2]^{13-}$ indicates that the hopping of a d^1 electron between WO_6 octahedra is the predominant deactivation channel of the $\text{O} \rightarrow \text{W}$ charge-transfer levels, which reduces drastically the communication with the excited levels of Eu^{3+} .

Upon photoexcitation of the ligand-to-metal charge-transfer (l.m.c.t.) bands of polyoxometalates, an electron is transferred to an orbital of d character at higher energy simultaneously with the creation of a vacancy in an oxygen orbital of $2p$ character at low energy. In the solid-state photochemistry of alkylammonium polyoxomolybdates the presence of a peculiar type of perturbation of the $\text{O} \rightarrow \text{Mo}$ l.m.c.t. states [equation (1)] has been demonstrated,¹⁻⁶ in which photoexcitation of the $\text{O} \rightarrow \text{Mo}$



l.m.c.t. band induces transfer of a hydrogen-bonding proton from an alkylammonium nitrogen to a bridging oxygen atom at the photoreducible site in the edge-shared MoO_6 octahedral lattice. This is followed by interaction of the electron in the high-energy d -type level with the proton. Simultaneous interaction of the hole with non-bonding electrons at the amino nitrogen atom leads to formation of a charge-transfer complex (I). This complex reflects the charge separation between the electron and the hole which are localized at the MoO_6 octahedron in the polyoxomolybdate lattice. The extent of delocalization of the d^1 electron has been related to the $\text{M}-\text{O}-\text{M}$ bond angle associated with the $d_{\pi}-p_{\pi}-d_{\pi}$ orbital mixing in the polyoxometalates.⁷⁻¹¹ In edge-shared MoO_6 octahedral lattices with $\text{Mo}-\text{O}-\text{Mo}$ bond angles of $87-118^\circ$ the d^1 electron is almost localized at a single MoO_6 octahedron site.^{1,5,6} On the other hand, in the Keggin framework with corner-sharing linking of different M_3O_{13} groups, thermally activated electron-hopping delocalization occurs between corner-shared MO_6 octahedra with $\text{M}-\text{O}-\text{M}$ bond angles of $142-155^\circ$.⁷⁻⁹ Furthermore, electron delocalization due to perfect orbital mixing takes place in the $\text{W}_{10}\text{O}_{32}$ lattice with approximately linear configurations ($\text{W}-\text{O}-\text{W}$ $176-177^\circ$) for the corner-shared WO_6 octahedra.^{10,11}

In the absence of a transferable proton (in the case of alkali-metal salts of polyoxometalates) a recombination between the electron and hole would follow photoexcitation of the $\text{O} \rightarrow \text{M}$ l.m.c.t. band, resulting in no chemical change. However, when there are several energy levels within the $\text{O} \rightarrow \text{M}$ l.m.c.t. bands, energy transfer occurs from the $\text{O} \rightarrow \text{M}$ l.m.c.t. excited state to these levels. This has been demonstrated for $[\text{Eu}(\text{W}_5\text{O}_{18})_2]^{9-}$ ^{9-12,15} where photoexcitation of the $\text{O} \rightarrow \text{W}$ l.m.c.t. band leads to energy transfer from $[\text{W}_5\text{O}_{18}]^{6-}$ to Eu^{3+} followed by a characteristic luminescence of Eu^{3+} . Similar behaviour has been reported for $[\text{Eu}(\text{SiW}_{11}\text{O}_{39})_2]^{13-}$ and $[\text{Eu}(\text{P}_2\text{W}_{17}\text{O}_{61})_2]^{17-13,16}$. From the standpoint of the preparation of other polyoxotungstoeuropates, it is important to note that all of the Eu^{3+} in these polyoxotungstoeuropates achieve eight-co-ordination to the lacunary derivatives of W_5O_{19} , Keggin $\text{SiW}_{12}\text{O}_{40}$, and Dawson $\text{P}_2\text{W}_{18}\text{O}_{62}$ structures. Thus, our interest in energy transfer involving the polyoxotungstate lattice has been focused on the polyoxotungstoeuropate containing trivacant Keggin-structure ligands. Recently, we have isolated a new luminescent polyoxotungstoeuropate complex, $\text{K}_{15}\text{H}_3[\text{Eu}_3(\text{H}_2\text{O})_3(\text{SbW}_9\text{O}_{33})(\text{W}_5\text{O}_{18})_3] \cdot 25.5\text{H}_2\text{O}$ (I), and investigated its luminescence properties, to understand the relaxation process of the $\text{O} \rightarrow \text{M}$ l.m.c.t. excitation in polyoxotungstoeuropate lattices. The structure of the complex has been characterized by single-crystal X -ray diffraction. This study of the intramolecular energy transfer from the $\text{O} \rightarrow \text{M}$ l.m.c.t. excited state to Eu^{3+} provides an insight at the molecular level since the polyoxometalates can be regarded as molecular fragments of an infinite metal oxide lattice.

Experimental

Preparation and Chemical Analysis.—All the reagents required for the preparation were used without further purification. The salts $\text{Na}_9[\text{Eu}(\text{W}_5\text{O}_{18})_2] \cdot 18\text{H}_2\text{O}$ and $\text{K}_{13}[\text{Eu}$

† Supplementary data available: see Instructions for Authors, *J. Chem. Soc., Dalton Trans.*, 1990, Issue 1, pp. xix–xxii.

Non-S.I. unit employed: eV $\approx 1.60 \times 10^{-19}$ J.

(SiW₁₁O₃₉)₂·3H₂O were prepared as described by Peacock and Weakley.¹⁷ The complex K₁₅H₃[Eu₃(H₂O)₃(SbW₉O₃₃)(W₅O₁₈)₃]·25.5H₂O (1) was prepared by the following method. Tungsten(vi) oxide (4.0 g) and KOH (2.5 g) were dissolved in water (30 cm³) on warming. Antimony(III) oxide (0.8 g) and Eu(NO₃)₃·6H₂O (0.4–0.5 g) in 12 mol dm⁻³ HCl (4.0 cm³) were added dropwise with stirring. The mixture was then kept at room temperature for 30 min, following by filtration. The clear colourless filtrate (at pH 7.4) was kept at 15 °C. Within 3 d white crystals were formed, accompanied by other crystalline phases that are non-luminescent. Luminescent crystals of (1) were removed from the solution under 395-nm light. After alkaline degradation, tungsten and potassium were determined by atomic absorption spectrometry at 400.9 and 766.5 nm, respectively. Antimony (Sb^{III}) was determined by a polarographic method (dropping mercury electrode) in 1 mol dm⁻³ NaOH at 1.15 V vs. Ag–AgCl. Europium was determined by back-titration with MnSO₄ in the presence of 0.01 mol dm⁻³ ethylenediaminetetra-acetate, NH₃–NH₄Cl buffer (pH 10), and eriochrome black T indicator.¹⁷ Thermogravimetric analysis (Rigaku, Thermoflex TG-DGC) was used for the determination of water of crystallization (Found: Eu, 6.10; K, 9.65; Sb, 1.25; W, 52.70; H₂O, 4.20. Calc. for H₆₀Eu₃K₁₅O_{115.5}SbW₂₄: Eu, 6.10; K, 7.85; Sb, 1.60; W, 59.0; H₂O, 6.15%). An attempt to synthesize other polyoxotungstoeuropates containing AsW₉O₃₃ or BiW₉O₃₃ moieties was unsuccessful.

Crystallography.—The crystals of complex (1) are monoclinic. Oscillation and Weissenberg photographs suggested the space group C2/m. Accurate unit-cell parameters were determined by least-squares treatment of angular co-ordinates of 15 reflections with 2θ = 15–25° measured with a Rigaku four-circle diffractometer.

Crystal data. H₆₀Eu₃K₁₅O_{115.5}SbW₂₄, *M* = 7 485.9, monoclinic, space group C2/m, *a* = 30.250(7), *b* = 18.568(5), *c* = 22.101(6) Å, β = 109.19(8)°, *U* = 11 723(5) Å³, *Z* = 4, *D*_c = 4.243 g cm⁻³, *F*(000) = 13 155, μ(Mo-K_α) = 248.2 cm⁻¹.

Intensities were collected in the range 2 < 2θ < 60° for a crystal with approximate dimensions 0.07 × 0.35 × 0.40 mm, using graphite-monochromatized Mo-K_α (λ = 0.710 69 Å) radiation and the ω–2θ scan technique at a 2θ scan rate of 8° min⁻¹. Lorentz and polarization corrections were applied and an absorption correction was made using the program DABEX.¹⁸ Correction factors were from 2.468 to 9.094. Of 10 677 independent reflections, 8 642 having *I* > 3σ(*I*), were retained for the structure refinement. The positions of the W atoms were obtained by a direct method using MULTAN 78.¹⁹ The atomic scattering factors and anomalous dispersion terms were taken from ref. 20. Calculations were carried out on the HITAC M-280H computer at this Institute. The structure was refined using the SHELX 76 package of programs.²¹ The quantity minimized was Σw(*F*_o – *F*_c)². The refinement converged to *R* = 0.125 and *R*' = 0.164 {*w* = Σ[σ²(*F*_o) + 0.0116*F*_o²]⁻¹} for 462 parameters. No extinction coefficient was applied. The maximum and minimum heights in the final difference synthesis were 9.8 and –8.4 e Å⁻³ respectively, around W atom at a distance of less than 1 Å. The high values of *R* and *R*' could be ascribed to poor crystal quality in addition to a high absorption index (μ = 248.2 cm⁻¹) and non-spherical crystals; the crystals lost water readily as they were taken from their solution. The atomic co-ordinates for the non-hydrogen atoms are listed in Table 1.

Additional material available from the Cambridge Crystallographic Data Centre comprises thermal parameters and remaining bond distances and angles.

Spectroscopy.—Sample powders were prepared by grinding

single crystals of complex (1) in an agate mortar. Diffuse reflection and i.r. spectra were recorded on Hitachi 330 and Jasco IRA-2 spectrophotometers, respectively. Emission and excitation spectra were obtained using a lock-in (NF L1-574) technique. A Hamamatsu TV R636 photomultiplier tube, connected to a Nikon G-25 grating monochromator, was used to detect emitted light. The wavelength dependence of the emission in the steady state of irradiation with a 500-W xenon lamp was determined and the signals obtained at λ < 400 nm were corrected to a constant photon flux at each wavelength. Measurements at 77 and 4.2 K were carried out using a liquid-nitrogen Dewar flask and an Oxford Instruments cryostat (CF 204), respectively. The exciting light was focused onto the sample, and the emitted light collected at an angle of 90° and focused onto the entrance slit of the monochromator. The time profiles of the luminescence from the ⁵D₀ state of Eu³⁺ under excitation with a pulsed NRG 0.9-5-90 nitrogen laser (337 nm) were obtained with a Sony-Tektronix 475 oscilloscope or a Kawasaki electronika MR-100E + TMC-400 signal averager. The emission quantum yields were evaluated by the method of Haas and Stein²² using as a standard Na₉[Eu(W₅O₁₈)₂]·18H₂O (φ = 0.80)²³ for 310-nm excitation. High-resolution emission spectra were recorded on a Jasco CT-1000 D double monochromator using the nitrogen laser for excitation. High-resolution excitation spectra were obtained with a Moletron DL-14P dye laser pumped by a Moletron UV-24 nitrogen laser. The high-resolution spectra were recorded with a slit width resolution of 1 cm⁻¹ and measurements of the *f*–*f* emission lines were recorded with an accuracy of ±2 cm⁻¹.

Results

Structure of K₁₅H₃[Eu₃(H₂O)₃(SbW₉O₃₃)(W₅O₁₈)₃]·25.5H₂O, (1).—A central trinuclear Eu₃(H₂O)₃ core in the anion is linked tetrahedrally by three W₅O₁₈ groups and one B-α type SbW₉O₃₃ group.²⁴ The anion of approximate point symmetry C_{3v} has a mirror plane through W(1), W(11), W(12), W(14), Sb, and Eu(2), as shown in Figure 1. The W₅O₁₈ group, which is known as part of [Ce(W₅O₁₈)₂]⁸⁻,²⁵ is the lacunary derivative of the W₆O₁₉ structure, a half moiety of [W₁₀O₃₂]⁴⁻.²⁶ The SbW₉ group is the trivacant Keggin structural B-α type ligand containing Sb^{III} having three-co-ordination²⁴ as in other polyoxotungstates where the XW₉O₃₃ moiety is of B-α type, notably [W₃(H₂O)₂(AsW₉O₃₃)₂]⁶⁻, [CoW₂O₂(H₂O)(AsW₉O₃₃)₂]⁸⁻, [Cu₃(H₂O)₃(AsW₉O₃₃)₂]¹²⁻, and [(Hg₂)₂WO(H₂O)(AsW₉O₃₃)₂]¹⁰⁻.^{27–29} This should be distinguished from the B-α XW₉O₃₄ moiety with tetrahedral XO₄ (X = Si^{IV}, Ge^{IV}, P^V, or As^V).^{30,31} Each Eu³⁺ in the Eu₃(H₂O)₃ core achieves eight-co-ordination by attachment of one W₅O₁₈ (four oxygens), one SbW₉O₃₃ (two oxygens), and two aqua ligands (two oxygens). Selected bond distance and angle data are shown in Table 2, hydrogen-bond distances and selected separations between heavy atoms in Table 3. The Eu(1)···Eu(2) and Eu(1)···Eu(1') distances are 5.067(4) and 5.015(5) Å, respectively. These are much larger than the Co···Co distances (3.16–3.31 Å) in [Co₄(H₂O)₂-(PW₉O₃₄)₂]¹⁰⁻ or Zn···Zn distances (3.24–3.46 Å) in [Zn₄(H₂O)₂(AsW₉O₃₄)₂]¹⁰⁻, where two Co or Zn atoms each carry a water ligand and the anion of crystallographic symmetry $\bar{1}$ contains two [XW₉O₃₄]⁹⁻ groups linked *via* four Co^{II}O₆ or Zn^{II}O₆ groups.³² The W–O bond distances in the W₅O₁₈ and SbW₉O₃₃ groups are little different from corresponding distances in [Ce(W₅O₁₈)₂]⁸⁻ or [W₁₀O₃₂]⁴⁻ and [M₄(H₂O)₂(XW₉O₃₄)₂]¹⁰⁻, respectively.^{25,26,32} The relative strength of the W–O, Eu–O, and Sb–O interactions is given in Table 4 where the bond strengths in valence units(*s*) are calculated using *s* = (*d*/1.904)^{-6.0}, (*d*/2.090)^{-6.5}, and (*d*/1.910)^{-4.5} for the W–O, Eu–O, and Sb–O bond lengths (*d*) in Å

Table 1. Atomic co-ordinates ($\times 10^4$ for W, Eu, Sb, and K; $\times 10^3$ for oxygen) for $K_{15}H_3[Eu_3(H_2O)_3(SbW_9O_{33})(W_5O_{18})]\cdot 25.5H_2O$ with estimated standard deviations (e.s.d.s) in parentheses

Atom	x	y	z	Atom	x	y	z
W(1)	2 106(1)	0	-264(1)	W(2)	1 486(1)	1 006(1)	686(1)
W(3)	3 096(1)	900(1)	521(1)	W(4)	1 943(1)	995(1)	2 293(1)
W(5)	2 489(1)	1 894(1)	1 451(1)	W(6)	5 202(1)	3 319(1)	3 052(1)
W(7)	4 975(1)	1 813(1)	3 713(1)	W(8)	4 179(1)	3 070(1)	3 291(1)
W(9)	4 213(1)	3 047(1)	1 829(1)	W(10)	5 001(1)	1 766(1)	2 245(1)
W(11)	2 906(1)	0	6 017(1)	W(12)	2 137(1)	0	4 538(1)
W(13)	2 948(1)	1 241(1)	4 942(1)	W(14)	3 760(1)	0	5 374(1)
Eu(1)	3 840(1)	1 350(1)	2 389(1)	Eu(2)	2 972(1)	0	3 646(1)
Sb	2 689(1)	0	1 659(2)	K(1)	3 104(4)	2 975(6)	491(6)
K(2)	2 948(7)	2 125(8)	3 233(8)	K(3)	4 078(8)	1 305(12)	4 347(8)
K(4)	1 556(10)	1 905(13)	3 915(13)	K(5)	3 802(11)	1 747(21)	6 578(22)
K(6)	4 939(6)	0	3 076(8)	K(7)	1 187(6)	0	2 985(8)
K(8)	4 239(6)	0	1 194(8)	K(9)	1 322(19)	0	-2 416(26)
K(10)	853(8)	0	-831(12)	O(2)	94(1)	128(2)	17(2)
O(1)	174(1)	0	-109(2)	O(4)	165(1)	130(1)	276(1)
O(3)	339(1)	148(1)	17(2)	O(6)	564(2)	401(2)	328(2)
O(5)	258(1)	281(2)	137(2)	O(8)	391(1)	366(2)	368(2)
O(7)	527(1)	141(2)	441(2)	O(10)	538(1)	136(2)	190(2)
O(9)	397(1)	360(1)	117(2)	O(12)	156(2)	0	433(3)
O(11)	286(2)	0	675(3)	O(14)	437(2)	0	577(2)
O(13)	294(1)	215(2)	506(2)	O(16)	254(1)	71(1)	-28(1)
O(15)	178(1)	68(1)	8(1)	O(18)	333(2)	0	31(3)
O(17)	134(1)	0	75(2)	O(20)	139(1)	114(1)	147(1)
O(19)	265(2)	0	71(3)	O(22)	267(1)	154(1)	73(1)
O(21)	183(1)	185(1)	78(1)	O(24)	222(1)	78(1)	146(1)
O(23)	215(1)	192(1)	208(2)	O(26)	542(1)	265(2)	376(2)
O(25)	176(1)	0	217(2)	O(28)	480(1)	363(1)	226(2)
O(27)	476(1)	369(2)	342(2)	O(30)	459(1)	251(1)	397(2)
O(29)	541(1)	260(2)	257(2)	O(32)	465(1)	244(2)	158(2)
O(31)	400(1)	353(1)	245(2)	O(34)	464(1)	248(1)	279(2)
O(33)	528(1)	142(2)	314(2)	O(36)	293(1)	97(2)	585(2)
O(35)	226(2)	0	549(2)	O(38)	227(1)	98(2)	467(2)
O(37)	358(2)	0	614(2)	O(40)	293(2)	0	496(3)
O(39)	361(1)	99(1)	534(2)	O(42)	297(1)	155(2)	196(2)
O(41)	348(1)	84(1)	135(1)	O(44)	449(1)	119(1)	337(1)
O(43)	249(1)	76(1)	280(1)	O(46)	379(1)	232(2)	171(2)
O(45)	378(1)	232(1)	306(1)	O(48)	226(1)	0	378(2)
O(47)	453(1)	112(1)	208(2)	O(50)	371(2)	0	456(2)
O(49)	300(1)	113(1)	413(2)	O(52)	354(1)	56(1)	316(2)
O(51)	389(1)	0	257(2)	O _w (2)	296(2)	90(3)	-122(3)
O _w (1)	134(3)	273(4)	220(4)	O _w (4)	555(2)	334(3)	154(3)
O _w (3)	271(4)	218(6)	635(6)	O _w (6)	21(3)	216(3)	-40(4)
O _w (5)	433(3)	150(4)	52(5)	O _w (8)	182(3)	121(4)	576(5)
O _w (7)	382(3)	261(5)	468(5)	O _w (10)	68(3)	0	166(5)
O _w (9)	368(3)	192(4)	-85(4)	O _w (12)	424(2)	0	727(3)
O _w (11)	510(4)	0	120(6)	O _w (14)	455(4)	500	385(6)
O _w (13)	442(3)	500	214(5)	O _w (16)	500	74(4)	0
O _w (15)	386(5)	500	419(6)				
O _w (17)	500	0	500				

respectively and the valence sum (bond order = Σs) of all W-O, Eu-O, or Sb-O bond strengths about a given oxygen or metal atom gives the valence of that atom.³³ The alternative expression, $s = \exp[(d_0 - d)/B]$, where d_0 and B are empirically determined parameters,³⁴ gave similar bond-valence values. The valence sums of the Eu-O bond strengths for O(51) and O(52) are 0.56(6) and 0.52(3) respectively, implying considerable negative charge on these atoms if they are not protonated. The values are in contrast to those, 1.4(3)—2.7(3), for all other oxygen atoms that carry formal negative charge in the W_5O_{18} and SbW_9O_{33} groups. In conjunction with the fact that the bond order [0.56(6) or 0.52(3)] for O(51) or O(52) is close to the value ($0.20 \times 2 = 0.40$)³⁵ predicted for the four-co-ordinated water oxygen in the crystal, the two protons can be located with a high degree of confidence on each of these bridging O(51) and O(52) atoms that are linked in the centre of

the anion *via* Eu atoms. Thus, atoms O(51), O(52), and O(52') comprise the diprotonated oxo bridges (aqua ligands) between Eu atoms, represented as $Eu_3(H_2O)_3$. The separations O(51)···O(52) 2.21(6) and O(52)···O(52') 2.08(7) Å are extraordinarily short compared with the O···O distances (2.41—2.49 Å³⁶) for the diaquahydrogen cation $[H_5O_2]^+$, excluding the possibility of the hydrogen bond in the $Eu_3(H_2O)_3$ core.

Taking into consideration both $Z = 4$ and the multiplicity of the Wyckoff position for each atom, the X-ray structural analysis indicates that complex (1) contains 15 K^+ cations and 25.5 lattice water oxygen (O_w) atoms. Figure 2 shows a half molecule with the numbering of the K^+ and O_w atoms. Atoms K(6)—K(10), $O_w(10)$ — $O_w(15)$, and $O_w(17)$ are situated on a crystallographic mirror plane. In addition, the O(28)··· $O_w(13)$, O(27)··· $O_w(14)$, and O(8)··· $O_w(15)$ separations, 2.77(11),

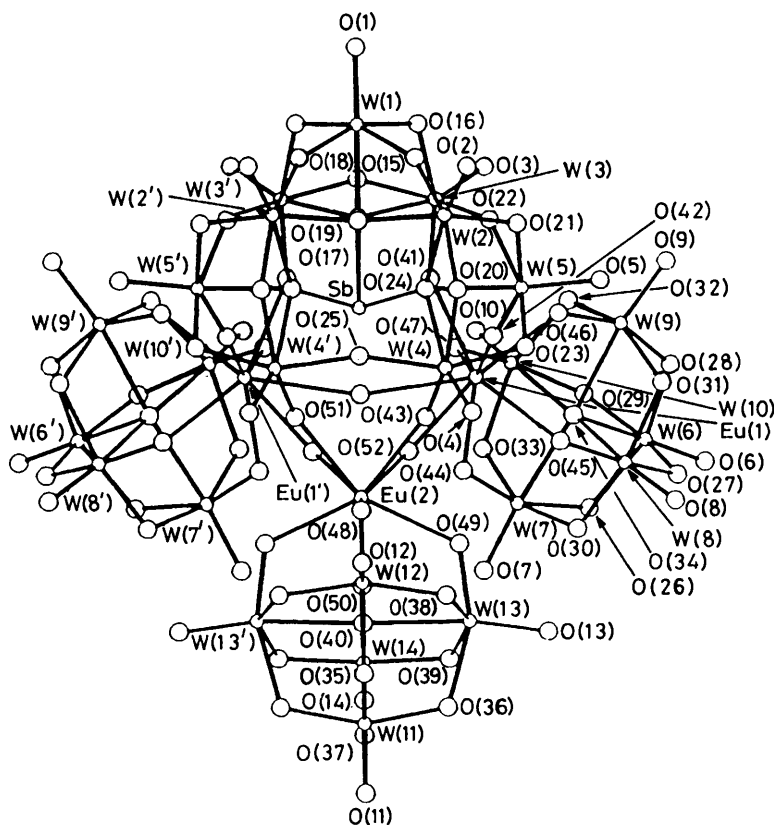


Figure 1. Structure of $[\text{Eu}_3(\text{H}_2\text{O})_3(\text{SbW}_9\text{O}_{33})(\text{W}_5\text{O}_{18})_3]^{18-}$ with the atom numbering scheme. Primed atoms are related to corresponding unprimed ones by a mirror plane

2.76(13), and 2.75(15) Å, respectively are comparable with the $\text{O}\cdots\text{O}$ distances of hydrogen-bonded water molecules, 2.70–2.80 Å.³⁷ Therefore it is possible to say that a pair of hydrogen bonds involving each of $\text{O}_w(13)$, $\text{O}_w(14)$, and $\text{O}_w(15)$ links neighbouring anions in the lattice (Table 3). Similarly, since $\text{O}_w(14)\cdots\text{O}_w(15)$ 2.45(19) and $\text{O}_w(6)\cdots\text{O}_w(6A)$ 2.50(16) Å are comparable to the $\text{O}\cdots\text{O}$ separation in $[\text{H}_5\text{O}_2]^+$, it is reasonable to assume that two protons in complex (1) belong to $[\text{H}_5\text{O}_2]^+$, considering the multiplicity of the Wyckoff position of $\text{O}_w(6)$, $\text{O}_w(14)$, and $\text{O}_w(15)$, eight, four, and four, respectively, in the unit cell. Then, (1) can be represented as $\text{K}_{15}[\text{H}_5\text{O}_2]_2\text{H}[\text{Eu}_3(\text{H}_2\text{O})_3(\text{SbW}_9\text{O}_{33})(\text{W}_5\text{O}_{18})_3]\cdot 21.5\text{H}_2\text{O}$.

Luminescence Properties.—The diffuse reflection spectrum of powdered complex (1) at 300 K is shown in Figure 3. The spectrum shows an intense broad absorption band with a maximum around 310 nm and a very weak and narrow band around 395 nm. The broad band can be assigned to $\text{O}\rightarrow\text{W}$ l.m.c.t. transitions of W_5O_{18} and $\text{SbW}_9\text{O}_{33}$ ligands which are practically unaffected by co-ordination. The $\text{O}\rightarrow\text{Eu}$ l.m.c.t. bands are expected to lie in the 240–250 nm region but are obscured by the intense polyoxotungstate bands, due to their small absorption coefficients.^{13,16} The narrow band around 395 nm corresponds to the ${}^7F_0\rightarrow{}^5L_6$ transition of Eu^{3+} ,¹⁶ which is superimposed on the tail of much more intense bands due to the W_5O_{18} and $\text{SbW}_9\text{O}_{33}$ ligands. The luminescence spectrum of the powder consists of ${}^5D_0\rightarrow{}^7F_J$ ($J=0-4$) transitions of Eu^{3+} ,³⁸ as shown in Figure 4 where the energies

of the ${}^5D_0\rightarrow{}^7F_J$ transitions in the high-resolution spectrum are given. Emission from the 5D_0 level is observed upon irradiation with u.v. and visible light at 300 K. The line at 579.5 nm corresponds to the ${}^5D_0\rightarrow{}^7F_0$ transition for the Eu^{3+} site, this transition being allowed for low symmetry (C_3) around the Eu^{3+} (Figure 1). Since both the 5D_0 and 7F_0 levels cannot be split by ligand-field effects, the observation of a single component in the ${}^5D_0\rightarrow{}^7F_0$ region under high-resolution conditions indicates that atoms $\text{Eu}(1)$ and $\text{Eu}(2)$ exhibiting crystallographically slightly different co-ordination (Table 2) can hardly be discriminated spectroscopically. Table 5 shows the relative intensities of ${}^5D_0\rightarrow{}^7F_J$ emission at 300 K for complex (1), $\text{Na}_9[\text{Eu}(\text{W}_5\text{O}_{18})_2]\cdot 18\text{H}_2\text{O}$, and $\text{K}_{13}[\text{Eu}(\text{SiW}_{11}\text{O}_{39})_2]\cdot 3\text{H}_2\text{O}$. The relative intensity of the ${}^5D_0\rightarrow{}^7F_2$ emission for (1), corresponding to the electronic dipole transition, is the highest. A decrease in temperature resulted in no significant change in the intensity ratio of the ${}^5D_0\rightarrow{}^7F_J$ emission.

The excitation spectra obtained at 300, 77, and 4.2 K are shown in Figure 5 where the emission is monitored for the most intense ${}^5D_0\rightarrow{}^7F_2$ transition at 613.1 nm. The spectra consist of broad bands corresponding to the transitions of the $\text{O}\rightarrow\text{W}$ l.m.c.t. of both W_5O_{18} and $\text{SbW}_9\text{O}_{33}$ ligands and a large number of lines due to the transition within the $4f^6$ configuration of Eu^{3+} . The intensity of the broad band increases with decreasing temperature. This indicates that the photoexcitation of the W_5O_{18} and $\text{SbW}_9\text{O}_{33}$ ligands is followed by energy transfer to the emitting 5D_0 state of Eu^{3+} and that this transfer takes place efficiently at low temperature. It may be noted that the position of the excitation maximum around 280 nm at 300 K [Figure 5(a)] is different from the absorption maximum around 310 nm (Figure 3). As supported by the relative increase in the excitation band around 310 nm with decreasing temperature (Figure 5), this is due to the well known phenomenon that in

* $\text{O}_w(6A)$ denotes atom $\text{O}_w(6)$ in the adjacent molecule at $-x, y, -z$ (Table 3).

Table 2. Selected bond lengths (Å) and angles (°) for $K_{15}H_3[Eu_3(H_2O)_3(SbW_9O_{33})(W_5O_{18})_3] \cdot 25.5H_2O$ with e.s.d.s in parentheses

W(1)–O(1)	1.78(4)	W(2)–O(2)	1.75(4)	W(3)–O(3)	1.73(3)
W(1)–O(15)	1.91(3)	W(2)–O(15)	1.93(3)	W(3)–O(16)	2.02(3)
W(1)–O(16)	1.88(3)	W(2)–O(17)	1.93(4)	W(3)–O(18)	1.94(7)
W(1)–O(19)	2.24(6)	W(2)–O(20)	1.85(3)	W(3)–O(19)	2.28(6)
		W(2)–O(21)	1.87(3)	W(3)–O(22)	1.91(3)
		W(2)–O(24)	2.34(3)	W(3)–O(41)	1.82(3)
W(4)–O(4)	1.66(3)	W(5)–O(5)	1.74(4)	W(6)–O(6)	1.79(5)
W(4)–O(20)	2.04(3)	W(5)–O(21)	2.06(3)	W(6)–O(26)	1.95(4)
W(4)–O(23)	1.95(3)	W(5)–O(22)	1.96(3)	W(6)–O(27)	1.91(4)
W(4)–O(24)	2.29(3)	W(5)–O(23)	1.98(3)	W(6)–O(28)	1.86(3)
W(4)–O(25)	1.92(4)	W(5)–O(24)	2.23(3)	W(6)–O(29)	1.93(4)
W(4)–O(43)	1.73(3)	W(5)–O(42)	1.65(4)	W(6)–O(34)	2.25(3)
W(7)–O(7)	1.68(4)	W(8)–O(8)	1.75(5)	W(9)–O(9)	1.73(3)
W(7)–O(26)	2.03(4)	W(8)–O(27)	2.03(4)	W(9)–O(28)	2.02(3)
W(7)–O(30)	1.94(4)	W(8)–O(30)	1.93(4)	W(9)–O(31)	1.92(3)
W(7)–O(33)	1.94(4)	W(8)–O(31)	1.95(3)	W(9)–O(32)	1.94(4)
W(7)–O(34)	2.32(3)	W(8)–O(34)	2.32(3)	W(9)–O(34)	2.34(3)
W(7)–O(44)	1.83(3)	W(8)–O(45)	1.81(3)	W(9)–O(46)	1.82(4)
W(10)–O(10)	1.74(4)	W(11)–O(11)	1.66(6)	W(12)–O(12)	1.66(6)
W(10)–O(29)	1.97(4)	W(11)–O(35)	1.92(5)	W(12)–O(35)	2.02(5)
W(10)–O(32)	1.96(4)	W(11)–O(36)	1.85(5)	W(12)–O(38)	1.86(4)
W(10)–O(33)	1.98(4)	W(11)–O(37)	1.97(5)	W(12)–O(40)	2.26(6)
W(10)–O(34)	2.30(3)	W(11)–O(40)	2.35(6)	W(12)–O(48)	1.83(4)
W(10)–O(47)	1.81(3)				
W(13)–O(13)	1.71(4)	W(14)–O(14)	1.77(5)	Sb–O(19)	2.05(6)
W(13)–O(36)	2.08(5)	W(14)–O(37)	1.94(5)	Sb–O(24)	1.98(3)
W(13)–O(38)	2.00(4)	W(14)–O(39)	1.90(3)		
W(13)–O(39)	1.96(3)	W(14)–O(40)	2.39(6)		
W(13)–O(40)	2.31(6)	W(14)–O(50)	1.75(6)		
W(13)–O(49)	1.87(3)				
Eu(1)–O(41)	2.40(3)	Eu(1)–O(46)	2.31(4)	Eu(2)–O(43)	2.40(3)
Eu(1)–O(42)	2.51(4)	Eu(1)–O(47)	2.43(3)	Eu(2)–O(48)	2.28(4)
Eu(1)–O(44)	2.41(3)	Eu(1)–O(51)	2.54(4)	Eu(2)–O(49)	2.34(3)
Eu(1)–O(45)	2.39(3)	Eu(1)–O(52)	2.64(3)	Eu(2)–O(50)	2.47(6)
				Eu(2)–O(52)	2.51(3)
W(1)–O(15)–W(2)	155(2)	W(2)–O(24)–W(5)	95(1)	W(9)–O(32)–W(10)	115(2)
W(1)–O(16)–W(3)	120(2)	W(2)–O(24)–Sb	137(1)	W(7)–O(33)–W(10)	113(2)
W(2)–O(17)–W(2')	150(2)	W(4)–O(24)–W(5)	94(1)	W(6)–O(34)–W(7)	94(1)
W(3)–O(18)–W(3')	119(4)	W(4)–O(25)–W(4')	148(3)	W(9)–O(34)–W(10)	90(1)
W(3)–O(19)–W(3')	94(2)	W(6)–O(26)–W(7)	114(2)	W(11)–O(36)–W(13)	116(2)
W(2)–O(20)–W(4)	119(1)	W(6)–O(27)–W(8)	116(2)	W(11)–O(37)–W(14)	117(2)
W(2)–O(21)–W(5)	119(2)	W(6)–O(28)–W(9)	119(2)	W(12)–O(38)–W(13)	116(2)
W(3)–O(22)–W(5)	143(2)	W(6)–O(29)–W(10)	118(2)	W(14)–O(39)–W(13)	116(2)
W(4)–O(23)–W(5)	115(2)	W(7)–O(30)–W(8)	115(2)	W(11)–O(40)–W(12)	93(2)
W(2)–O(24)–W(4)	93(1)	W(8)–O(31)–W(9)	115(2)	W(14)–O(40)–W(13)	88(2)
W(3)–O(41)–Eu(1)	151(2)	W(9)–O(46)–Eu(1)	127(2)	Eu(1)–O(51)–Eu(1')	163(2)
W(5)–O(42)–Eu(1)	153(2)	W(10)–O(47)–Eu(1)	122(2)	Eu(1)–O(52)–Eu(2)	159(2)
W(4)–O(43)–Eu(2)	149(2)	W(12)–O(48)–Eu(2)	127(2)		
W(7)–O(44)–Eu(1)	127(1)	W(13)–O(49)–Eu(2)	122(2)	O(19)–Sb–O(24)	88(2)
W(8)–O(45)–Eu(1)	125(2)	W(14)–O(50)–Eu(2)	126(3)	O(24)–Sb–O(24')	94(1)

strongly absorbing crystals excitation into the absorption maximum is not very effective because it cannot enter the crystal and considerable radiationless losses occur in the surface layer.^{13,39} Another feature of the temperature effect on the excitation spectrum is the disappearance of several sublines in each of the spectral ranges 589–595, 530–540, 468–478, and 414–420 nm at $T \leq 77$ K. The high-resolution excitation spectrum at 300 K can be resolved into several components as shown in Figure 6. The excitation spectrum in the ${}^7F_0 \rightarrow {}^5D_0$ region under high-resolution conditions (Figure 6) displays a single line and three components to low energy. The positions of these four lines at 17 247, 16 971, 16 855, and 16 807 cm^{-1} respectively

correspond to the emission lines for the ${}^5D_0 \rightarrow {}^7F_0$ (17 255 cm^{-1}) and ${}^5D_0 \rightarrow {}^7F_1$ (16 975 and $\approx 16 834$ cm^{-1}) transitions (Figure 4). Therefore, the three well separated bands to low energy may be assigned to the ${}^7F_1 \rightarrow {}^5D_0$ transition of the Eu^{3+} site having C_s symmetry. Upon cooling to 77 K the thermal population of the higher-energy 7F_1 state is substantially reduced due to the Boltzmann factor intensity-dependent changes with temperature, leaving the vast majority of Eu^{3+} in the 7F_0 level. Thus, the sublines to low energy for the other spectral region may be assigned to the transition from 7F_1 sublevels.

The 5D_0 emission decay ($\tau_{e.c.}$) after excitation into the O \rightarrow W

Table 3. Selected interatomic distances (Å) for $K_{15}H_3[Eu_3(H_2O)_3(SbW_9O_{33})(W_5O_{18})_3] \cdot 25.5H_2O$ with e.s.d.s in parentheses

K(1)···O(3)	3.05(4)	K(2)···O(23)	2.91(4)	K(3)···O(30)	2.99(4)	K(4)···O(4)	2.90(4)
K(1)···O(5)	2.92(4)	K(2)···O(42)	3.03(4)	K(3)···O(39)	3.03(4)	K(4)···O(38)	2.84(5)
K(1)···O(9)	2.81(4)	K(2)···O(43)	2.89(4)	K(3)···O(44)	2.83(4)	K(4)···O(6 ^{IV})	3.16(6)
K(1)···O(22)	3.10(4)	K(2)···O(45)	2.67(4)	K(3)···O(49)	3.16(4)	K(4)···O(13 ^{II})	2.88(5)
K(1)···O(46)	3.07(4)	K(2)···O(49)	2.67(4)	K(3)···O(50)	2.77(6)	K(4)···K(5 ^{II})	2.80(6)
K(1)···O(15 ^I)	2.88(3)	K(2)···O _w (3 ^{II})	2.78(13)	K(3)···O(52)	2.94(4)	K(4)···O _w (3 ^{II})	2.99(13)
K(1)···O(16 ^I)	3.06(3)			K(3)···O _w (7)	2.73(11)		
K(1)···O(21 ^I)	2.89(4)			K(3)···O(7 ^{III})	2.82(5)		
K(1)···O(22 ^I)	3.08(4)						
K(5)···O(36)	2.97(7)	K(6)···O(33)	2.82(4)	K(7)···O(4)	2.92(4)	K(8)···O(18)	2.80(7)
K(5)···O(39)	2.96(6)	K(6)···O(44)	2.78(4)	K(7)···O(12)	2.81(6)	K(8)···O(41)	2.89(3)
K(5)···O(29 ^{III})	2.97(6)	K(6)···O(47)	2.99(4)	K(7)···O(25)	2.89(5)	K(8)···O(47)	2.80(4)
K(5)···O(35 ^{III})	2.71(6)	K(6)···O(51)	3.00(5)	K(7)···O(48)	3.14(4)	K(8)···O _w (5)	3.21(10)
K(5)···O _w (1 ^{II})	3.04(10)	K(6)···O(14 ^{III})	2.71(6)	K(7)···O _w (10)	2.83(10)	K(8)···O(11)	2.59(13)
		K(6)···O _w (12 ^{III})	2.84(8)	K(7)···O(6 ^{IV})	2.70(5)		
K(9)···O(1)	2.80(7)	K(9)···O _w (13 ^I)	2.52(12)	K(10)···O(9)	2.81(4)	K(10)···O(1 ^V)	2.93(5)
K(9)···O(31 ^I)	2.90(7)			K(10)···O _w (13)	2.74(11)	K(10)···O(15 ^V)	3.13(4)
O _w (1)···O(4)	2.95(9)	O _w (5)···O(3)	2.68(11)	O _w (9)···O(3)	2.82(11)	O _w (14)···O(8)	3.10(13)
O _w (1)···O(23)	2.94(9)	O _w (5)···O(32)	2.83(11)	O _w (9)···O(21 ^I)	2.79(11)	O _w (14)···O(27)	2.76(13)
O _w (1)···O _w (9 ^I)	3.01(13)	O _w (5)···O _w (9)	3.13(14)			O _w (14)···O _w (15)	2.45(19)
O _w (1)···O _w (4 ^{IV})	3.09(12)	O _w (5)···O _w (16)	3.01(12)	O _w (10)···O(20)	3.15(11)	O _w (14)···O(8 ^{IX})	3.10(13)
		O _w (5)···O _w (6 ^I)	2.90(13)	O _w (10)···O(25)	3.08(11)	O _w (14)···O(27 ^{IX})	2.76(13)
O _w (2)···O(16)	2.78(7)	O _w (5)···O _w (16 ^{VIII})	3.01(12)				
O _w (2)···O _w (9)	2.79(12)			O _w (11)···O(10)	2.94(14)	O _w (15)···O(8)	2.75(15)
O _w (2)···O(5 ^I)	2.83(8)	O _w (6)···O(2)	2.71(9)	O _w (11)···O _w (16)	2.91(15)	O _w (15)···O(8 ^{IX})	2.75(15)
		O _w (6)···O(32 ^I)	2.88(9)	O _w (11)···O _w (16 ^{VII})	2.91(15)		
O _w (3)···O(13)	3.151(14)	O _w (6)···O _w (6 ^{VIII})	2.50(16)			O _w (16)···O _w (16 ^V)	2.74(14)
O _w (3)···O _w (8)	3.15(17)			O _w (12)···O(37)	2.64(9)		
		O _w (7)···O(8)	3.02(11)	O _w (12)···O(10 ^{III})	3.11(8)	O _w (17)···O(7)	3.15(4)
O _w (4)···O(28)	3.23(8)	O _w (7)···O(13)	3.15(11)			O _w (17)···O(14)	2.94(5)
O _w (4)···O(29)	2.81(9)	O _w (7)···O _w (8 ^{II})	2.86(15)	O _w (13)···O(28)	2.77(11)	O _w (17)···O(7 ^V)	3.15(4)
O _w (4)···O(32)	3.23(9)			O _w (13)···O(31)	3.19(11)	O _w (17)···O(14 ^V)	2.94(5)
O _w (4)···O _w (6 ^I)	2.94(11)	O _w (8)···O(35)	2.77(12)	O _w (13)···O(28 ^{IX})	2.77(11)	O _w (17)···O(7 ^{III})	3.15(4)
O _w (4)···O _w (10 ^{VI})	3.11(13)	O _w (8)···O(38)	3.16(11)	O _w (13)···O(31 ^{IX})	3.19(11)	O _w (17)···O(14 ^{III})	2.94(5)
O _w (4)···O(20 ^{VI})	2.78(8)	O _w (8)···O _w (15 ^{II})	3.08(18)			O _w (17)···O(7 ^{III})	3.15(4)
		O _w (8)···O(8 ^{II})	2.88(11)			O _w (17)···O(14 ^X)	2.94(5)
W(1)···W(2)	3.741(3)	W(6)···W(7)	3.331(3)	W(3)···Eu(1)	4.087(3)	O(41)···O(42)	2.71(5)
W(1)···W(3)	3.372(3)	W(6)···W(8)	3.340(3)	W(5)···Eu(1)	4.054(3)	O(41)···O(51)	3.00(5)
W(2)···W(4)	3.362(3)	W(6)···W(9)	3.344(3)	W(7)···Eu(1)	3.807(3)	O(42)···O(52)	3.22(5)
W(2)···W(5)	3.378(3)	W(7)···W(8)	3.263(3)	W(8)···Eu(1)	3.725(3)	O(43)···O(43 ^I)	2.82(5)
W(3)···W(5)	3.672(3)	W(7)···W(9)	4.648(3)	W(9)···Eu(1)	3.695(3)	O(43)···O(52)	3.01(5)
W(4)···W(5)	3.316(3)	W(7)···W(10)	3.274(3)	W(10)···Eu(1)	3.713(3)	O(44)···O(45)	2.92(4)
		W(8)···W(9)	3.267(3)			O(44)···O(47)	2.89(5)
W(1)···Sb	4.032(5)	W(8)···W(10)	4.603(3)	W(4)···Eu(2)	3.991(4)	O(45)···O(46)	3.00(5)
W(3)···Sb	3.561(4)	W(9)···W(10)	3.279(3)	W(12)···Eu(2)	3.680(5)	O(46)···O(47)	3.07(5)
W(4)···Sb	3.542(4)	W(11)···W(12)	3.331(4)	W(13)···Eu(2)	3.696(4)	O(48)···O(49)	2.98(5)
W(5)···Sb	3.572(4)	W(11)···W(13)	3.342(4)	W(14)···Eu(2)	3.779(4)	O(49)···O(50)	2.94(6)
		W(11)···W(14)	3.334(4)			O(51)···O(52)	2.21(6)
Eu(1)···Sb	4.161(5)	W(12)···W(13)	3.269(4)	Eu(2)···O(51)	4.21(4)	O(52)···O(52 ^I)	2.08(7)
Eu(2)···Sb	4.188(5)	W(12)···W(14)	4.643(4)				
Eu(1)···Eu(2)	5.067(4)	W(13)···W(13 ^I)	4.609(3)				
Eu(1)···Eu(1 ^I)	5.015(5)	W(13)···W(14)	3.274(4)				

Symmetry codes: I $\frac{1}{2} - x, \frac{1}{2} - y, -z$; II $\frac{1}{2} - x, \frac{1}{2} - y, 1 - z$; III $1 - x, y, 1 - z$; IV $-\frac{1}{2} + x, \frac{1}{2} - y, z$; V $x, -y, z$; VI $\frac{1}{2} + x, \frac{1}{2} - y, z$; VII $1 - x, y, -z$; VIII $-x, y, -z$; IX $x, 1 - y, z$; X $1 - x, -y, 1 - z$.

l.m.c.t. level shows exponential behaviour and $\tau_{c.t.} = 1.1 \pm 0.2$ ms is almost temperature-independent. The value is shorter than for $Na_9[Eu(W_5O_{18})_2]$ (3.3 ms) and $K_{13}[Eu(SiW_{11}O_{39})_2]$ (2.4 ms). The quantum efficiency ($\phi_{c.t.}$) of the luminescence under O \rightarrow W l.m.c.t. excitation at 300 nm is 0.25 at 300 K and increases with decreasing temperature (0.51 and 0.55 at 77 and 4.2 K, respectively). Table 6 lists $\tau_{c.t.}$ and $\phi_{c.t.}$ for the three complexes.

Discussion

Figure 7 shows a schematic representation of the EuO_8 site of local C_s symmetry. The average Eu–O bond distances are 2.52, 2.37, and 2.46 Å for SbW_9O_{33} , W_5O_{18} , and aqua oxygen atoms, respectively. Since O(44)···O(45), O(45)···O(46), O(46)···O(47), O(47)···O(44), O(48)···O(49), and O(49)···O(50) are 2.92(4), 3.00(5), 3.07(5), 2.89(5), 2.98(5), and 2.94(6) Å respectively, four oxygen atoms belonging to a W_5O_{18}

Table 4. Sum of metal–oxygen bond strengths about a given atom *

W(1)	6.0(7)	O(1)	1.5(2)	O(18)	1.8(4)	O(35)	1.7(2)
W(2)	6.1(7)	O(2)	1.7(2)	O(19)	1.8(3)	O(36)	1.8(3)
W(3)	6.0(7)	O(3)	1.8(2)	O(20)	1.8(2)	O(37)	1.7(2)
W(4)	6.8(8)	O(4)	2.2(2)	O(21)	1.7(2)	O(38)	1.9(3)
W(5)	6.7(7)	O(5)	1.7(2)	O(22)	1.8(2)	O(39)	1.8(2)
W(6)	5.8(8)	O(6)	1.5(2)	O(23)	1.6(2)	O(40)	1.4(3)
W(7)	6.0(5)	O(7)	2.1(3)	O(24)	1.8(2)	O(41)	1.7(2)
W(8)	5.8(8)	O(8)	1.7(3)	O(25)	1.9(3)	O(42)	2.7(4)
W(9)	5.9(6)	O(9)	1.8(2)	O(26)	1.5(2)	O(43)	2.1(3)
W(10)	5.9(7)	O(10)	1.7(3)	O(27)	1.7(2)	O(44)	1.7(2)
W(11)	6.8(12)	O(11)	2.3(5)	O(28)	2.0(2)	O(45)	1.8(2)
W(12)	6.9(10)	O(12)	2.3(5)	O(29)	1.7(2)	O(46)	1.8(3)
W(13)	5.5(7)	O(13)	1.9(3)	O(30)	1.8(3)	O(47)	1.7(2)
W(14)	6.5(10)	O(14)	1.5(2)	O(31)	1.8(2)	O(48)	1.9(3)
Eu(1)	2.9(3)	O(15)	1.9(2)	O(32)	1.7(3)	O(49)	1.6(1)
Eu(2)	3.3(3)	O(16)	1.8(2)	O(33)	1.7(2)	O(50)	2.0(4)
Sb	2.4(2)	O(17)	1.8(2)	O(34)	1.6(1)	O(51)	0.56(6)
						O(52)	0.52(3)

* The standard errors given in parentheses refer to the last decimal place given.

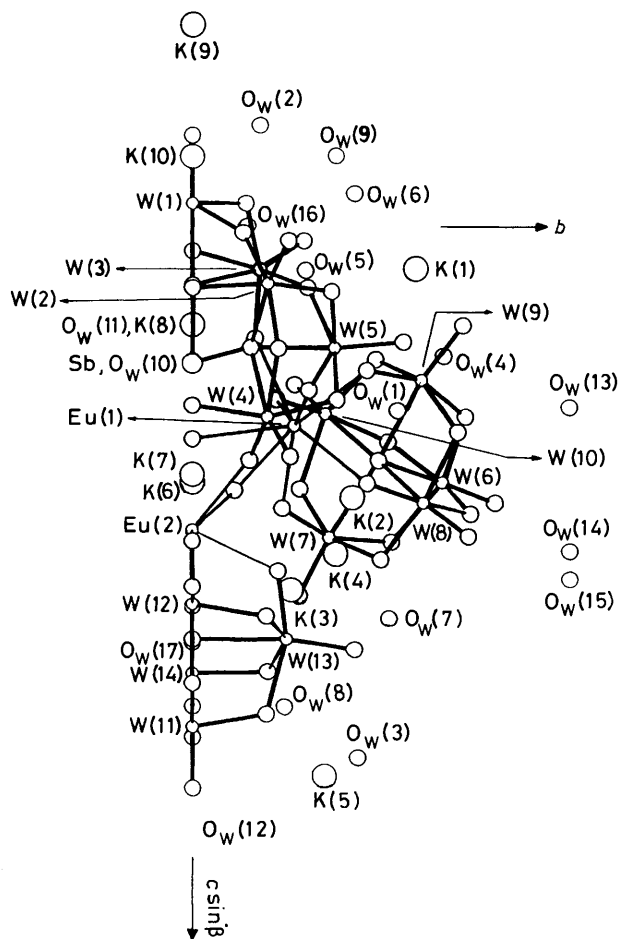


Figure 2. Structure of half a molecule of $K_{15}H_3[Eu_3(H_2O)_3(SbW_9O_{33})(W_5O_{18})_3] \cdot 25.5H_2O$, viewed in projection along the a axis

ligand at the EuO_8 site lie approximately at the positions of a square plane. On the other hand, since $O(41) \cdots O(42)$, $O(42) \cdots O(52)$, $O(52) \cdots O(51)$, $O(51) \cdots O(41)$, $O(43) \cdots O(52)$, $O(52) \cdots O(52')$, and $O(43) \cdots O(43')$ are 2.71(5), 3.22(5), 2.21(6), 3.00(5), 3.01(5), 2.08(7), and 2.82(5) Å respec-

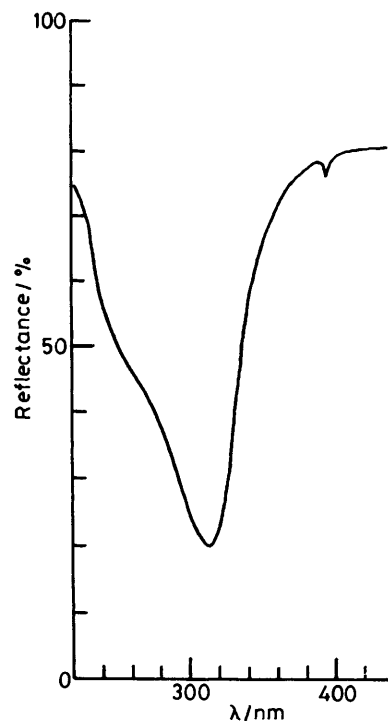


Figure 3. Diffuse reflection spectrum of complex (1) at 300 K

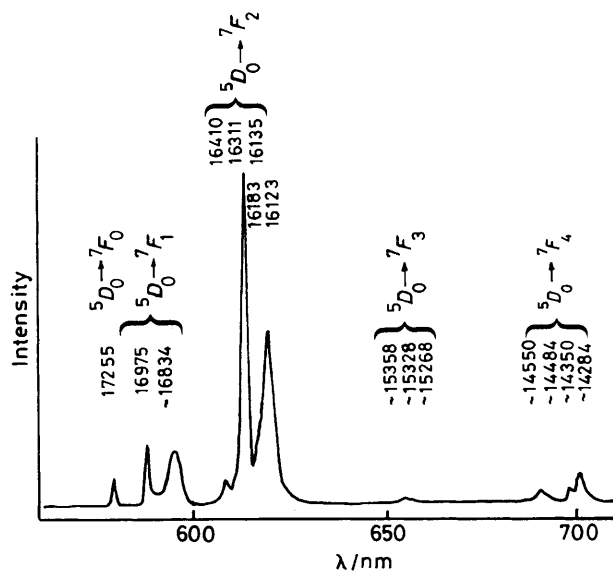


Figure 4. Emission spectrum of complex (1) at 300 K under low resolution. The positions of ${}^5D_0 \rightarrow {}^7F_J$ ($J = 0-4$) emission lines under high resolution are indicated in frequency units

Table 5. Relative intensities of the ${}^5D_0 \rightarrow {}^7F_J$ emissions of Eu^{3+} in polyoxotungstates at 300 K *

Terminal level	(1)	$Na_9[Eu(W_5O_{18})_2]$	$K_{13}[Eu(SiW_{11}O_{32})_2]$
7F_0	5	≈ 0	2
7F_1	16	61	39
7F_2	66	26	43
7F_3	3	3	4
7F_4	11	10	13

* The intensity is calculated with respect to the total intensity of the ${}^5D_0 \rightarrow {}^7F_J$ ($J = 0-4$) transitions.

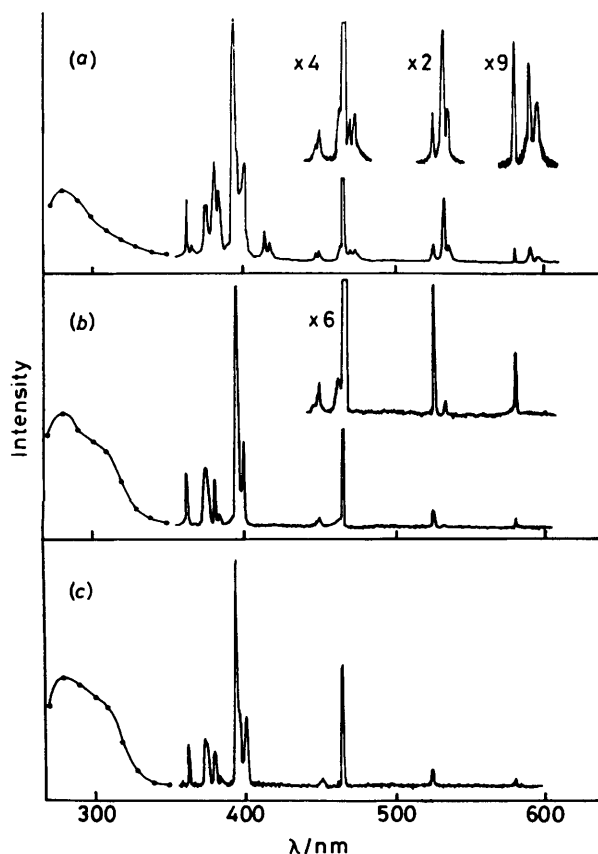


Figure 5. Excitation spectra of complex (1) at 300 (a), 77 (b), and 4.2 K (c) under low resolution. Analyzing wavelength 613.1 nm ($^5D_0 \rightarrow ^7F_2$ transition)

tively, each two oxygen atoms belonging to $\text{SbW}_9\text{O}_{33}$ and aqua ligands deviate significantly from a square-planar arrangement. The angles $\text{Eu}(1)\cdots\text{Eu}(2)\cdots\text{Eu}(1')$, $\text{Eu}(2)\cdots\text{Eu}(1)\cdots\text{Eu}(1')$, $\text{O}(52)\cdots\text{O}(51)\cdots\text{O}(52')$, and $\text{O}(51)\cdots\text{O}(52)\cdots\text{O}(52')$ are 59, 60, 56, and 62°, respectively. The sum of the six O–Eu–O and Eu–O–Eu angles in the $\text{Eu}_3(\text{H}_2\text{O})_3$ core is 630° and the dihedral angle between the two planes $\text{Eu}(1)\text{Eu}(2)\text{Eu}(1')$ and $\text{O}(52)\text{O}(52')\text{O}(51)$ is 3.5°. The deviation from a planar arrangement for Eu and aqua oxygen atoms arises from distortion due to the co-ordination of the non-equivalent ligands W_5O_{18} , $\text{SbW}_9\text{O}_{33}$, and H_2O . The average O...O distance between the pair of aqua O atoms now bridged by a Eu atom and the average Eu...Eu distance is 2.17 and 5.05 Å, respectively. These distances are significantly different from corresponding average O...O (3.05 Å) and Zr...Zr (4.13 Å) distances in $[\text{Zr}_3(\text{OH})_3(\text{SiW}_9\text{O}_{34})_2]^{11-}$ where the Zr atoms are linked in the equatorial plane *via* hydroxo oxygen atoms and the overall co-ordination geometry is close to trigonal prismatic, the local three-fold axis of the ZrO_6 group lying in the equatorial plane.⁴⁰

The temperature effect on the intramolecular energy transfer from the excited level of the O→W l.m.c.t. for the ligands to the emitting 5D_0 level of Eu^{3+} depends strongly on the structure of the ligands (Table 6): $\phi_{\text{c.t.}}$ for $\text{K}_{13}[\text{Eu}(\text{SiW}_{11}\text{O}_{39})_2]$ at 295 K drops by a factor larger than 10^3 compared with that at 77 K, whereas complex (1) and $\text{Na}_9[\text{Eu}(\text{W}_5\text{O}_{18})_2]$ give moderate values of $\phi_{\text{c.t.}}$ with a smaller effect of temperature. It can be recalled that the thermal activation energy for electron hopping in the corner-sharing WO_6 octahedral lattice is much less than in the edge-sharing WO_6 lattice, 0.004 and 0.06 eV having been reported for $[\text{BW}_{12}\text{O}_{40}]^{6-}$ and $[\text{W}_{10}\text{O}_{32}]^{5-}$, respectively.^{7,11}

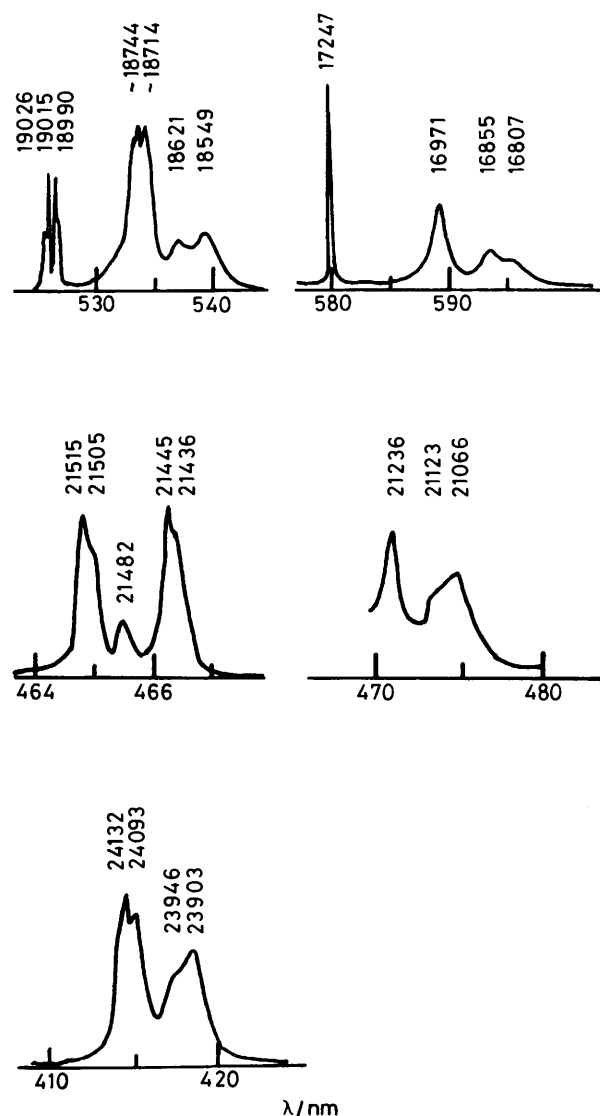


Figure 6. High-resolution excitation spectra of complex (1) at 300 K. Analyzing wavelength 613.1 nm. Vertical scales are not directly comparable

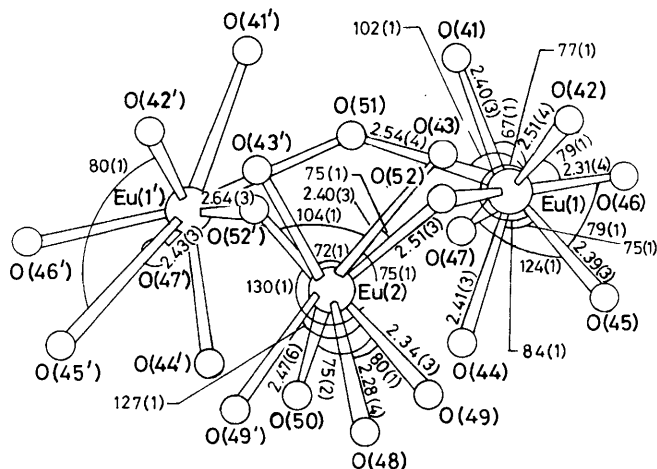


Figure 7. Bond distances (Å) and angles (°) in the $\text{Eu}_3(\text{H}_2\text{O})_3$ core of complex (1)

Table 6. The 5D_0 emission decay ($\tau_{c.t.}$) and emission quantum yield ($\phi_{c.t.}$) upon excitation of the O→W l.m.c.t. band

Polyoxotungstate powder	$\tau_{c.t.}/\text{ms}$			$\phi_{c.t.}$			$10^{-2}\phi_{c.t.}/\tau_{c.t.}/\text{s}^{-1}$		
	300	77	4.2 K	300	77	4.2 K	300	77	4.2 K
(1)	1.1 ± 0.2	1.1 ± 0.2	1.1	0.25	0.51	0.55	2.3	4.6	5.0
$\text{Na}_9[\text{Eu}(\text{W}_5\text{O}_{18})_2]$	2.8*	3.3*	—	0.80*	0.9*	—	2.9*	2.7	—
$\text{K}_{13}[\text{Eu}(\text{SiW}_{11}\text{O}_{39})_2]$	2.4*	2.7*	—	$<10^{-3} \cdot 1^*$	—	—	$<4 \times 10^{-3}$	3.7	—

* Ref. 16. Values for room temperature are at 295 K.

Thus, the hopping delocalization of a d^1 electron must occur more predominantly in $\text{SbW}_9\text{O}_{33}$ or $[\text{XW}_{11}\text{O}_{39}]^{n-}$ ligands involving the corner-sharing WO_6 octahedral configuration with W–O–W bond angles of about 150° than in the W_5O_{18} ligand with five edge-shared WO_6 octahedra and W–O–W bond angles of about 100° . Therefore, it is reasonable to assume that the electron delocalization among WO_6 octahedra is the deactivation channel of the O→W l.m.c.t. energy, which would reduce the communication between O→W l.m.c.t. levels and excited Eu^{3+} levels drastically. In other words, a large degree of the localization of the d^1 electron induced by the O→W l.m.c.t. band photoexcitation at a WO_6 octahedron must be readily followed by energy transfer from the excited level of the O→W l.m.c.t. state to Eu^{3+} . The temperature effect on $\phi_{c.t.}$ (Table 6) can then be explained by the Boltzmann factor for the electron hopping. As shown in Table 6, complex (1) gives an increase in $\phi_{c.t.}/\tau_{c.t.}$ with decreasing temperature (2.3×10^2 , 4.6×10^2 , and $5.0 \times 10^2 \text{ s}^{-1}$ at 300, 77, and 4.2 K respectively), whereas with $\text{Na}_9[\text{Eu}(\text{W}_5\text{O}_{18})_2]$ there is little effect of temperature on $\phi_{c.t.}/\tau_{c.t.}$ (2.9×10^2 and $2.7 \times 10^2 \text{ s}^{-1}$ at 295 and 77 K, respectively). This indicates that energy transfer from the W_5O_{18} ligand in (1) occurs exclusively at 300 K and that the additional energy transfer from the $\text{SbW}_9\text{O}_{33}$ ligand contributes to the emission at low temperature. The average volume of a molecule of complex (1) ($11\,723/4 = 2\,930.8 \text{ \AA}^3$) is approximately two times larger than that ($6\,214/4 = 1\,553 \text{ \AA}^3$) of a molecule of $\text{Na}_9[\text{Eu}(\text{W}_5\text{O}_{18})_2]$, if the crystal structure of the latter is assumed to be isomorphous with that of $\text{Na}_6\text{H}_2[\text{CeW}_{10}\text{O}_{36}] \cdot 30\text{H}_2\text{O}$ (space group $C2/c$, $Z = 4$, $U = 6\,214 \text{ \AA}^3$).²⁵ Therefore, the light intensity absorbed by the unit polyoxotungstate moiety in the crystals of both (1) (containing four polyoxotungstate ligands) and $\text{Na}_9[\text{Eu}(\text{W}_5\text{O}_{18})_2]$ (containing two polyoxotungstate ligands) would be nearly equal, but the concentration of Eu^{3+} in (1) would be 1.5 times higher than for $\text{Na}_9[\text{Eu}(\text{W}_5\text{O}_{18})_2]$. Since $\phi_{c.t.} = 0.80$ at 295 K for the latter is based on the energy transfer from the two W_5O_{18} ligands,¹³ the quantum yield based on the energy transfer from the W_5O_{18} ligands of (1) may be $(1/2) \times 0.80 \times 1.5 = 0.60$. However, $\phi_{c.t.} = 0.25$ at 300 K (Table 6) is not necessarily explained by the negligible energy transfer from the $\text{SbW}_9\text{O}_{33}$ ligand. In conjunction with the fact that $\tau_{c.t.}$ for complex (1) is appreciably shorter than for both $\text{Na}_9[\text{Eu}(\text{W}_5\text{O}_{18})_2]$ and $\text{K}_{13}[\text{Eu}(\text{SiW}_{11}\text{O}_{39})_2]$ which have no aqua ligand in the first coordination sphere of Eu^{3+} ,^{14,16} an additional reason for the smaller $\phi_{c.t.}$ for (1) is radiationless deactivation of the 5D_0 level by two aqua ligands, probably by coupling with the high-frequency OH oscillators.³⁸ From the radiative transition rate at Eu^{3+} , which is close to $5.0 \times 10^2 \text{ s}^{-1}$ ($= \phi_{c.t.}/\tau_{c.t.}$ at 4.2 K), the rate of non-radiative decay by the aqua ligands could be estimated as $4 \times 10^2 \text{ s}^{-1}$ ($= 1/\tau_{c.t.} - 5.0 \times 10^2$), if the rate of other radiationless decay from the 5D_0 level of (1) is almost the same ($<1 \times 10^2 \text{ s}^{-1}$) as for $\text{Na}_9[\text{Eu}(\text{W}_5\text{O}_{18})_2]$. As suggested by $\phi_{c.t.} = 1$ for $\text{K}_{13}[\text{Eu}(\text{SiW}_{11}\text{O}_{39})_2]$ at 77 K (Table 6),¹⁶ the efficient energy transfer from the O→W l.m.c.t. excited state for the large ligand of the lacunary Keggin polyoxotungstate implies that the energy transfer from the O→W l.m.c.t. excited

state in the polyoxotungstate lattice to Eu^{3+} occurs at least over 6.9 Å, which corresponds to the distance of atoms W(1) and W(2) in the $\text{SbW}_9\text{O}_{33}$ ligand from the nearest Eu atom, W(1)···Eu(1) (6.93 Å) and W(2)···Eu(1) (6.90 Å). The lack of detectable emission from the ligands of complex (1) supports the conclusion that the radiative transition rate (10^5 s^{-1}) at the polyoxotungstate group is much lower than the transfer rate (at least 10^7 s^{-1}) to Eu^{3+} .¹³

Acknowledgements

We are indebted to Professors Y. Ohashi and Y. Sasada for providing facilities for X-ray measurements and valuable advice. Thanks are also due to Professor T. Hirose and Mr. N. Akamatsu for providing facilities for high-resolution emission and excitation spectra measurements.

References

- 1 T. Yamase and M. Suga, *J. Chem. Soc., Dalton Trans.*, 1989, 661.
- 2 T. Yamase, *J. Chem. Soc., Dalton Trans.*, 1982, 1987.
- 3 T. Yamase, *J. Chem. Soc., Dalton Trans.*, 1985, 2585.
- 4 T. Yamase, *Polyhedron*, 1986, 5, 79.
- 5 M. Isobe, F. Marumo, T. Yamase, and T. Ikawa, *Acta Crystallogr., Sect. B*, 1978, 34, 2728.
- 6 Y. Ohashi, K. Yanagi, Y. Sasada, and T. Yamase, *Bull. Chem. Soc. Jpn.*, 1982, 55, 1254.
- 7 T. Yamase and R. Watanabe, *J. Chem. Soc., Dalton Trans.*, 1986, 1669.
- 8 C. Sanchez, J. Livage, J. P. Launay, M. Fournier, and Y. Jeannin, *J. Am. Chem. Soc.*, 1982, 104, 3194.
- 9 C. Sanchez, J. Livage, J. P. Launay, and M. Fournier, *J. Am. Chem. Soc.*, 1983, 105, 6817.
- 10 T. Yamase, *J. Chem. Soc., Dalton Trans.*, 1987, 1597.
- 11 T. Yamase and T. Usami, *J. Chem. Soc., Dalton Trans.*, 1988, 183.
- 12 M. J. Stillman and A. J. Thompson, *J. Chem. Soc., Dalton Trans.*, 1976, 1138.
- 13 G. Blasse, G. J. Dirksen, and F. Zonnevijlle, *J. Inorg. Nucl. Chem.*, 1981, 43, 2847; *Chem. Phys. Lett.*, 1981, 83, 449.
- 14 R. Ballardini, Q. G. Mulazzani, M. Venturi, F. Bolletta, and V. Balzani, *Inorg. Chem.*, 1984, 23, 300.
- 15 J. R. Darwent, C. D. Fint, and P. J. O'Grady, *Chem. Phys. Lett.*, 1986, 127, 547.
- 16 R. Ballardini, E. Chiorboli, and V. Balzani, *Inorg. Chim. Acta*, 1984, 95, 323.
- 17 R. D. Peacock and T. J. R. Weakley, *J. Chem. Soc. A*, 1971, 1836.
- 18 S. Ohba, 'Manual for CHAGE System,' ed. T. Itoh, Computer Center of Tokyo University, Tokyo, 1986, p. 22.
- 19 P. Main, S. E. Hull, L. Lessinger, G. Germain, J. P. Declercq, and M. M. Woolfson, MULTAN 78, A System of Computer Programs for the Automatic Solution of Crystal Structures from X-ray, Diffraction Data, University of York, York, 1978.
- 20 'International Tables for X-Ray Crystallography,' Kynoch Press, Birmingham, 1974, vol. 4, pp. 99 and 149; D. T. Cromer and D. Liberman, *J. Chem. Phys.*, 1970, 53, 1891.
- 21 G. M. Sheldrick, SHELX 76, Program for Crystal Structure Determination, University of Cambridge, 1976.
- 22 Y. Haas and G. Stein, *J. Phys. Chem.*, 1971, 75, 3668.
- 23 G. Blasse, G. J. Dirksen, and F. Zonnevijlle, *Chem. Phys. Lett.*, 1981, 83, 449.

- 24 R. Constant, J-M. Fruchard, G. Hervé, and A. Tézé, *C.R. Acad. Sci., Ser. C*, 1974, **278**, 199.
- 25 J. Iball, J. N. Low, and T. J. R. Weakley, *J. Chem. Soc., Dalton Trans.*, 1974, 2021.
- 26 Y. Sasaki, T. Yamase, Y. Ohashi, and Y. Sasada, *Bull. Chem. Soc. Jpn.*, 1987, **60**, 4285; J. Fuchs, H. Hartl, W. Schiller, and U. Gerlach, *Acta Crystallogr., Sect. B*, 1976, **34**, 740.
- 27 Y. Jeannin and J. Martin-Frère, *J. Am. Chem. Soc.*, 1981, **103**, 1664; *Inorg. Chem.*, 1984, **23**, 3394.
- 28 T. J. R. Weakley, *Inorg. Chim. Acta*, 1984, **87**, 13.
- 29 F. Robert, M. Leyrie, and G. Hervé, *Acta Crystallogr., Sect. B*, 1982, **38**, 358.
- 30 G. Hervé and A. Tézé, *Inorg. Chem.*, 1977, **16**, 2115; R. G. Finke, B. Rapko, R. J. Saxton, and P. J. Domaille, *J. Am. Chem. Soc.*, 1986, **108**, 2947; R. G. Finke, M. W. Droegge, and P. J. Domaille, *Inorg. Chem.*, 1987, **26**, 3886.
- 31 C. Tourné, A. Revel, G. Tourné, and M. C. Vendrell, *C.R. Acad. Sci., Ser. C*, 1973, **277**, 643.
- 32 H. T. Evans, C. M. Tourné, G. F. Tourné, and T. J. R. Weakley, *J. Chem. Soc., Dalton Trans.*, 1986, 2699.
- 33 I. D. Brown and K. K. Wu, *Acta Crystallogr., Sect. B*, 1976, **32**, 1957.
- 34 D. Altermatt and I. D. Brown, *Acta Crystallogr., Sect. B*, 1985, **41**, 240; I. D. Brown and D. Altermatt, *ibid.*, p. 144.
- 35 I. D. Brown, 'Structure and Bonding in Crystals,' vol. 2, eds. M. D. Keffe and A. Navrotsky, Academic Press, New York, 1981, p. 1.
- 36 J. Emsley, *Chem. Soc. Rev.*, 1980, **9**, 91.
- 37 J. O. Lundgren and I. Olovsson, *J. Chem. Phys.*, 1968, **49**, 1063; J. M. Williams and S. W. Peterson, *J. Am. Chem. Soc.*, 1969, **91**, 776.
- 38 G. Blasse, 'Handbook on the Physics and Chemistry of Rare Earths,' vol. 4, eds. K. A. Gschneidner, jun., and L. Eyring, North-Holland, Amsterdam, 1979, p. 209; W. D. Horrocks, jun., and D. K. Sudnick, *Acc. Chem. Res.*, 1981, **14**, 384; V. Balzani, N. Sabbatini, and F. Scandola, *Chem. Rev.*, 1986, **86**, 319.
- 39 Z. Mazurak, G. Blasse, and J. Liebertz, *J. Solid State Chem.*, 1987, **68**, 181.
- 40 R. G. Finke, B. Rapko, and T. J. R. Weakley, *Inorg. Chem.*, 1989, **28**, 1573.

Received 25th July 1989; Paper 9/03126J